

ORIGINAL ARTICLE**Formulation and Evaluation of Dual-Release Inlay Tablet for Artesunate and Amodiaquine Hydrochloride: A Novel Approach to Malaria Treatment****Nilesh S. Mhaske*, Pallavi Dahiphale**¹Department of Pharmaceutical Quality assurance, Dr. Vithalrao Vikhe Patil Foundation's College of Pharmacy, Ahmednagar, Maharashtra 414111, India.***Corresponding author's email:** nilesh.2273@gmail.com**ABSTRACT**

The study aimed to develop and optimize a dual-release inlay tablet combining artesunate for immediate release and amodiaquine hydrochloride for sustained release to enhance therapeutic efficacy, reduce dosing frequency, and improve patient compliance in malaria treatment. A Central Composite Design (CCD), a factorial design-based optimization approach, was employed to assess the influence of ethyl cellulose and HPMC K4M on tablet hardness and drug release. Analytical methods such as UV spectrophotometry, FTIR, DSC, and MTT assay were used for characterization. The optimized batch was evaluated for drug content, release kinetics, cytotoxicity, and stability. The optimized formulation (PF8) contained 12.92% ethyl cellulose and 7.5% HPMC K4M. It exhibited hardness of 6.54 ± 0.04 kg/cm² and 98.9% drug release of amodiaquine at 12 hours. Artesunate released $97.8 \pm 1.1\%$ within 30 minutes. Release kinetics followed first-order ($R^2 = 0.9979$) and Hixson-Crowell ($R^2 = 0.9827$) models. The formulation remained stable over 3 months and showed an IC₅₀ value of 114.61 µg/mL in THP-1 cells, indicating a safe cytotoxicity profile. The dual-release inlay tablet demonstrated robust mechanical, release, and stability profiles with potential for improved malaria therapy. Its synchronized drug release and favorable safety suggest strong prospects for clinical translation, subject to validation through in vivo studies.

Keywords: Dual-release inlay tablet; Artesunate; Amodiaquine hydrochloride; Central Composite Design; Drug release kinetics; Malaria therapy; Stability study; MTT assay.

Received 18.09.2025

Revised 24.10.2025

Accepted 26.11.2025

How to cite this article:

Nilesh S. M, Pallavi D. Formulation and Evaluation of Dual-Release Inlay Tablet for Artesunate and Amodiaquine Hydrochloride: A Novel Approach to Malaria Treatment. Adv. Biores. Vol 16 [6] November 2025. 199-216

INTRODUCTION

It was estimated that in 2021, malaria caused 247 million cases and about 619,000 deaths, mostly in sub-Saharan Africa [1]. Keeping up with the medical costs and loss of work because of the disease is estimated to cost the economy more than USD 12 billion each year [2]. In spite of having antimalarial therapies, problems such as drug resistance, incomplete elimination of the parasite and patients not following the treatment plan make controlling malaria difficult. Traditional combination therapies are usually effective, yet drug differences can result in drugs' effects not working as well which may allow the infection to come back [3]. Drug not being released at a consistent speed also results in fluctuations in the bloodstream which can raise the chance of resistance. New developments recommend finding better ways to provide medicine that allows medicines to be released at the same time, helps more medicine be absorbed by the body and makes patients more likely to follow the treatment plan [4]. New drug formulation techniques could tackle these difficulties, but few have been successfully brought to the market. So, novel approaches that boost the drug interactions between antimalarial agents must be developed [5].

Artesunate, a substance made from artemisinin, is strong in fighting malaria and destroys the parasite Plasmodium falciparum rapidly, even in drug-resistant cases [6]. The sesquiterpene lactone structure with the key endoperoxide bridge in its center helps produce reactive oxygen species that damage proteins in the parasite [7]. Artemisinin derivatives such as artesunate, clear from the bloodstream in

under 30 minutes, so they are often given together with other drugs to be effective for longer [8]. The antimalarial Amodiaquine hydrochloride works with Artesunate because an active metabolite of Amodiaquine, desethylamodiaquine, helps protect against malaria after treatment [9]. The technique stops the multiple heme formation inside the parasite food organ which results in the parasite dying. There is evidence that taking both artesunate and amodiaquine together greatly decreases the risk of treatment failure more than using a single drug only. At present, conventional strategies for mixing do not consider the pharmacokinetic differences among the drugs which points to the need for an approach that ensures equal drug release for maximum effectiveness [10].

To face these difficulties, a dual-release inlay tablet of artesunate and amodiaquine hydrochloride is proposed in this current study [11]. Diptisol has a quick dissolving peel with artesunate that starts working right away, while a core made of amodiaquine hydrochloride remains active over a longer period [12]. It works because artesunate removes the parasites rapidly and amodiaquine helps maintain a long-lasting presence, ensuring the patient's parasites are always being suppressed. Advances in polymers and new matrix compression techniques allow for better control over drug release which boosts how much of the medicine reaches the body and reduces the frequency of dosing [13]. With dual-release systems, pharmacists can provide better matching of drugs in the body, more consistent taking of medicine by patients and possible resistance reduction [14]. Using inlay tablet designs for chronic diseases has been successful and using the same concept for treating malaria could lead to new and valuable outcomes. Using current manufacturing processes and using local resources can reduce costs and help the device be used in more places [15].

The purpose of this study is to develop and test a new inlay tablet that releases artesunate and amodiaquine hydrochloride together to enhance how malaria is treated. Certain aims are creating a reliable formulation, describing its physical and chemical characteristics, studying drug release examining the pharmacokinetic matching of drugs. Its purpose is to improve drug treatment, improve how much patients are able to take their medicine and create a workable solution for places with a lot of malaria.

MATERIAL AND METHODS

Materials

Artesunate and Amodiaquine Hydrochloride were obtained from ChemoX Laboratories (India). HPMC K4M, Ethyl Cellulose, MCC, SSG, PVP K30, starch, talc, aerosil, and magnesium stearate were procured from Loba Chemie and S.D. Fine Chem Ltd. (India). All solvents and reagents used were of analytical grade and purchased from Merck. The THP-1 cell line was obtained from NCCS (Pune, India), and cell culture reagents including DMEM, FBS, Trypsin-EDTA, and MTT reagent were sourced from HiMedia (Mumbai, India).

Methods

Determination of scanning absorbance maxima (λ_{\max})

Using a Jasco V630 UV-Visible spectrophotometer from Jasco Inc. (located in Tokyo, Japan), the maximum absorbance wavelengths (λ_{\max}) for artesunate and amodiaquine hydrochloride were found. Stock solutions (100 $\mu\text{g/mL}$) were diluted 10 times using methanol to make 10 $\mu\text{g/mL}$ standard solutions. The compounds were scanned between 200 and 400 nm using quartz cuvettes (length of 1 cm) filled with methanol as a blank. λ_{\max} was recorded for each drug and all the observations were made in triplicate ($n=3$) [16,17].

Calibration curve determination

Each of these standard stock solutions contained 100 μg of artesunate and amodiaquine hydrochloride per milliliter. From a stock of artesunate, 0.5, 1.0, 1.5, 2.0, 2.5- and 3.0-mL solution was taken and diluted in methanol to fill each 10 mL volumetric flask to reach concentrations of 5, 10, 15, 20, 25 and 30 $\mu\text{g/mL}$. Among dilutions for amodiaquine hydrochloride, 1.0, 2.0, 3.0, 4.0 and 5.0 mL were diluted to 10 mL to yield 10, 20, 30, 40 and 50 $\mu\text{g/mL}$. Both absorbance measurements were done using quartz cuvettes (1 cm path length) at their λ_{\max} point; the measurements were referenced to methanol. A plot was made for each drug's calibration curve and every sample was tested three times ($n=3$) [18,19].

Determination of solubility

Artesunate and amodiaquine hydrochloride were tested for their solubility with the solvent saturation technique. Sampling mixtures were prepared by adding a large amount of each PERKO drug to 10 mL of different solvents, including distilled water, methanol, ethanol, acetone, dimethyl sulfoxide (DMSO) and phosphate buffer pH 6.8 in closed glass vials. The shaker was set to $25 \pm 2^\circ\text{C}$ and 100 rpm and the vials were shaken for 48 hours to allow equilibrium to be set. The liquid from the mixtures was filtered using Whatman filter paper No. 1 and the filtrate was diluted with methanol. The amount of drug in the formulation was determined by looking at absorbance at the wavelength with the strongest reading for

each drug and then the results were measured in mg/mL of solution. All of the tests were repeated three times (n=3) [20,21].

Differential scanning calorimetry (DSC)

Differential scanning calorimetry was run to determine how artesunate, amodiaquine hydrochloride, the ingredients used and their combination reacted with heat. About 5 mg of each sample was put into an aluminum pan, weighed and analyzed by a DSC instrument (Mettler Toledo DSC 3+) with a nitrogen purge. Samples were heated with a ramp of 10°C per minute, starting at 30°C and going up to 300°C, using a continuous nitrogen flow of 50 mL/min. An empty aluminum pan served as the reference. Through thermograms, melting points, phase transitions and potential interactions could be observed. All experiments were done three times (n=3) [22,23].

Fourier Transform Infrared Spectroscopy (FTIR)

Artesunate, amodiaquine hydrochloride, some excipients and their mixture were analyzed by Fourier transform infrared spectroscopy to look for interaction possibilities. Using a Bruker Alpha II FTIR spectrophotometer (made in Germany), the spectra were taken over an area from 4000 to 400 cm⁻¹ using the method of KBr pellets. For each sample, about 2 mg was mixed with 200 mg of dry KBr, turned into a transparent disc by the hydraulic press and scanned at a resolution of 4 cm⁻¹. Functional groups in the molecule could be detected from specific peaks seen in each spectrum. All measurements were done three times each (n=3) [24].

Experimental design

A Central Composite Design (CCD) was employed for the systematic optimization of dual-release inlay tablets, using Design-Expert software version 13.0 (Stat-Ease Inc., USA). The formulation matrix included two independent formulation variables: ethyl cellulose (X₁), varied from 15% to 25% w/w, and hydroxypropyl methylcellulose K4M (X₂), varied from 5% to 10% w/w. A total of 13 experimental runs were generated, incorporating factorial points, axial points, and center points, with the latter fixed at level 5 to ensure model robustness and to assess experimental error. The dependent responses evaluated were in-vitro drug dissolution at 12 hours (Y₁) and tablet hardness (Y₂), both critical attributes reflecting the sustained-release and mechanical integrity of the formulation, respectively. The design allowed comprehensive analysis of the main effects, interaction effects, and quadratic effects of the selected variables on the performance characteristics of the tablets. The coded and actual levels of the independent and dependent variables are summarized in Table 1. The general form of the second-order polynomial equation used to model the relationship between the independent variables (X₁ and X₂) and the response variables (Y) is as follows:

$$Y = \beta_0 + \beta_1X_1 + \beta_2X_2 + \beta_{12}X_1X_2 + \beta_{11}X_1^2 + \beta_{22}X_2^2$$

Where: Y = predicted response, β_0 = intercept, β_1 , β_2 = linear coefficients, β_{12} = interaction coefficient β_{11} , β_{22} = quadratic coefficients, X₁, X₂ = independent variables (ethyl cellulose and HPMC K4M) [25].

Table 1: Variables and their Levels in Central Composite Design

Variables	Levels	
Independent variables	Low	High
(A) = Ethyl Cellulose (% w/w)	15	25
(B) = HPMC K4M (% w/w)	5	10
Dependent variables	Goals	
(R ₁) = In-vitro Drug Dissolution at 12 hr (%)	Maximize	
(R ₂) = Hardness (Kg/cm ²)	Maximize	

Formulation of Dual-Release Inlay Tablets

The dual-release inlay tablet was formulated in two stages: an immediate-release layer containing artesunate and a sustained-release core containing amodiaquine hydrochloride. For the immediate-release layer, artesunate was blended with sodium starch glycolate, microcrystalline cellulose, starch, aerosil, and magnesium stearate in quantities as shown in Table 2. For the sustained-release core, amodiaquine hydrochloride was blended with HPMC K4M, ethyl cellulose, lactose, PVP K30, starch, talc and magnesium stearate as shown in Table 3. All ingredients were passed through a #60 sieve and mixed uniformly. The core tablets were compressed first using a single-punch tablet machine (Rimek Mini Press-I, Karnavati Engineering, India), followed by addition of the artesunate blend and recompression to obtain inlay tablets. All formulations were prepared in batches of 100 tablets under controlled temperature and humidity conditions [26].

Table 2: Composition of Immediate Release Layer of Artesunate in % w/w

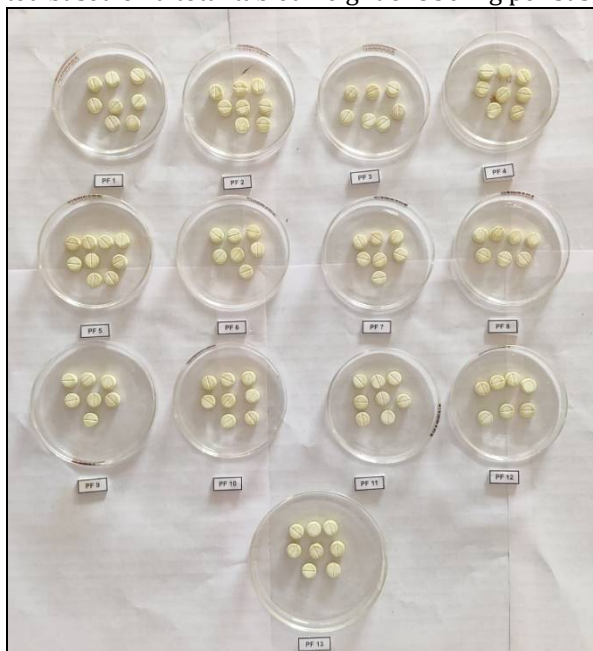
Ingredient	PF1	PF2	PF3	PF4	PF5	PF6	PF7	PF8	PF9	PF10	PF11	PF12	PF13
Artesunate	33.33	33.33	33.33	33.33	33.33	33.33	33.33	33.33	33.33	33.33	33.33	33.33	33.33
Sodium Starch Glycolate	9.53	6.83	5.90	15.13	5.80	18.40	13.67	23.17	5.07	16.10	6.10	23.67	9.73
MCC	46.85	53.35	54.52	45.05	53.05	41.11	46.51	37.01	55.35	44.08	54.08	36.51	50.45
Starch	5.33	5.33	5.33	5.33	5.33	5.33	5.33	5.33	5.33	5.33	5.33	5.33	5.33
Aerosil	0.25	0.25	0.25	0.25	0.25	0.25	0.25	0.25	0.25	0.25	0.25	0.25	0.25
Magnesium Stearate	0.90	0.90	0.90	0.90	0.90	0.90	0.90	0.90	0.90	0.90	0.90	0.90	0.90

All percentages are calculated based on a total tablet weight of 150 mg per immediate release layer.

Table 3: Composition of Sustained Release Core of Amodiaquine HCl

Ingredient	PF1	PF2	PF3	PF4	PF5	PF6	PF7	PF8	PF9	PF10	PF11	PF12	PF13
Amodiaquine HCl	42.86	42.86	42.86	42.86	42.86	42.86	42.86	42.86	42.86	42.86	42.86	42.86	42.86
HPMC K4M	7.50	5.00	5.00	7.50	7.50	3.96	11.04	7.50	10.00	7.50	7.50	7.50	10.00
Ethyl Cellulose	20.00	15.00	25.00	27.07	20.00	20.00	20.00	12.93	25.00	20.00	20.00	20.00	15.00
Lactose	19.16	6.87	11.54	15.14	29.49	15.14	18.86	19.23	26.03	22.29	18.89	5.23	19.14
PVP-K30	5.00	5.00	5.00	5.00	5.00	5.00	5.00	5.00	5.00	5.00	5.00	5.00	5.00
Starch	5.00	5.00	5.00	5.00	5.00	5.00	5.00	5.00	5.00	5.00	5.00	5.00	5.00
Magnesium Stearate	0.71	0.71	0.71	0.71	0.71	0.71	0.71	0.71	0.71	0.71	0.71	0.71	0.71
Talc	1.00	1.00	1.00	1.00	1.00	1.00	1.00	1.00	1.00	1.00	1.00	1.00	1.00

All percentages are calculated based on a total tablet weight of 350 mg per sustained release core tablet.

**Figure 1: All formulated batches of Dual-Release Inlay Tablets**

Evaluation of Dual-Release Inlay Tablets

Organoleptic Evaluation

A sample of the final batch of dual-release inlay tablets was examined visually and smelled by our team to check its color, smell and how it looks. Each tablet was looked at carefully for uniform color and shape and it was checked to see if it had any noticeable cracks, mottling or chipping. The smell was checked by putting a tablet to the nose and smelling it gently. These parameters were checked visually and by use of the senses to guarantee that the final result is pleasant to taste and smell, as prescribed by Indian Pharmacopoeia [27].

Tablet Weight Variation

Five tablets were taken randomly from each set of dual-release inlay tablets and their weights were measured one by one using a calibrated digital analytical balance. An average tablet weight was calculated and every tablet's weight was matched to see if it matched. The weight of each tablet for tablets above 250 mg should be not more than 5% below or above the average as required by Indian Pharmacopoeia. A batch is successful if not more than two tablets differ from the mean by more than the stated limit and none differ from the mean by more than twice the limit [28].

Tablet Thickness and Diameter

Dual-release inlay tablets were randomly selected and their thickness and diameter were measured using a calibrated Vernier caliper. Both measurements, thickness and diameter, were taken in millimeters by putting each tablet between the caliper's jaws and recording the readings. Every effort was made to keep the tablet from being compressed when it was handled for measurements. All results were given as mean values plus or minus the standard deviation. If the tablets are uniform in thickness and shape, it shows good compression and contributes to easy packaging, good interaction with blisters and equal amounts of medicine in each tablet [29].

Tablet Hardness and Friability

Hardness and friability were tested in dual-release inlay tablets to see how mechanically strong they are. Hardness tests for each batch were conducted using ten tablets and a Monsanto-type hardness tester and the results were recorded in kg/cm^2 . The mean hardness and standard deviation were computed so that the material could stand up well to handling and use. A Roche friabilator was used to assess friability by having ten pre-weighed tablets rotate for 4 minutes and 100 revolutions at 25 rpm. The tablets were reweighed after dusting and the percentage by which they lost weight was determined. Tablets are said to be friable enough according to the Indian Pharmacopoeia if the maximum weight loss is just 1%, showing they are strong enough for use and transportation [30].

Disintegration Time (for Immediate Release Layer)

Using an apparatus referred to in the Indian Pharmacopoeia, the time it took for the immediate release layer in dual-release inlays to disintegrate was studied. Individually, six tablets were put into the tubes of the basket rack assembly and the rest of the apparatus was used with distilled water kept at $37 \pm 2^\circ\text{C}$. The tablets were constantly exposed to raising and lowering and the amount of time when each tablet turned into pieces of coating alone was noted. A value for the average disintegration time was determined [31].

Drug Content Uniformity

Artesunate and amodiaquine hydrochloride concentration were examined in the dual-release inlay tablets separately with a UV-Vis spectrophotometry method. Individual weights were measured for ten tablets from every batch. Every tablet was crushed into a fine powder and the amount listed on the container was carefully measured out and put into a 100 mL volumetric flask. Methanol was added and the solution was sonicated for 30 minutes to guarantee that all of the drug came out, then filtered through Whatman filter paper No. 1. After being properly diluted, the filtrate was measured with a UV spectrophotometer at the right λ_{max} values for each pigment. Using the standard calibration curve, we figured out the amount of drug in each tablet and we stated the results as a percentage of what was labeled on the container [32].

In-vitro Drug Dissolution Study

Tests on the drug dissolution of the dual-release inlay tablets in the USP Type II (paddle) device were performed. The test for the immediate-release artesunate was done in 900 mL 0.1 N HCL maintained at $37 \pm 0.5^\circ\text{C}$ with 50 rpm paddle stirring. Withdrawn samples were filtered and analyzed using spectrophotometry at the specific wavelength of artesunate (λ_{max}) at five time points: 5, 10, 15, 20 and 30 minutes. A sustained-release core with amodiaquine hydrochloride was tested in the phosphate buffer (6.8 pH) medium for 12 hours, with samples collected at predetermined times (1, 2, 4, 6, 8, 10 and 12 hours). After taking each sample, fresh buffer was added to make sure sink conditions were preserved. At every chosen time, the drug levels released were measured using an existing calibration curve. In order to be precise, each experiment was repeated three times and the results were plotted as a line on a chart showing drug release over time [33].

Release Kinetics Modelling

The in-vitro drug release profiles of both artesunate (immediate release layer) and amodiaquine hydrochloride (sustained release core) were subjected to kinetic modeling using zero-order, first-order, Higuchi, and Korsmeyer-Peppas equations. The analysis was carried out using Microsoft Excel to

determine the release mechanism and rate for each drug. The model showing the best correlation coefficient (R^2) was considered to represent the drug release behavior [34].

In-vitro cell cytotoxicity study

MTT assays were done on THP-1 human monocytic cells to determine the cytotoxicity of Artesunate. A total of 10% fetal bovine serum and the standard temperature of 37°C and a 5% concentration of CO₂ were used for growing THP-1 cells in DMEM under normal conditions. One million cells were seeded in each well of a 96-well plate and the plate was left in the incubator for 24 hours to let them adhere. The cells were next subjected to nine concentrations of filter-sterilized Artesunate which were prepared by halving the concentration twice in MEM along with FBS. All control wells were incubated with culture medium alone, not with the test item. Within 48 hours after incubation, morphological changes became visible when observing through an inverted microscope. Subsequently, 10 µL of MTT reagent was poured into every well and then the plates were incubated for another 4 hours to let the formazan crystals develop. The plates were shaken for about one hour while being kept at room temperature after adding 100 µL of the solubilization solution. Every sample's absorbance was measured at 570 nm on a microplate reader and cell survival was worked out as a percentage based on the results from untreated cells. The IC₅₀ was found by plotting log concentration against percent survival using GraphPad Prism software [35].

Stability Studies

Optimized dual-release tablets were examined to find out how they would behave chemically and physically under fast testing. The tablets were kept in high-density polyethylene containers and stored at a temperature of 40 to 42°C and a relative humidity of 75 to 77% for 3 months, according to the ICH Q1A(R2) guidelines. At 0, 1, 2 and 3 months, some samples were collected and checked for their appearance, how easily they could be broken, hardness, content of active substances, toys breaking down after a set time point and how long it took for both layers to release their respective drugs during testing. They compared the results to the initial values to see if anything had changed [36].

Statistical Analysis

Statistical analysis was carried out using Design Expert version 13.0 and GraphPad Prism software to evaluate the influence of ethyl cellulose and HPMC K4M on in-vitro drug dissolution at 12 hours and tablet hardness. Design Expert was used for ANOVA, model fitting, and response surface analysis, while GraphPad Prism assisted in plotting release profiles and calculating mean ± SD. A p-value less than 0.05 was considered statistically significant for all tests [43].

RESULTS AND DISCUSSION

Results

Results of scanning absorbance maxima

The UV-visible spectrophotometric analysis confirmed the λ_{max} of Artesunate at 227 nm and Amodiaquine Hydrochloride at 342 nm in methanol. These well-defined absorbance peaks were used as the detection wavelengths for quantitative evaluation of the drugs. The respective UV spectra are shown in Figure 2A for Artesunate and Figure 2B for Amodiaquine Hydrochloride.

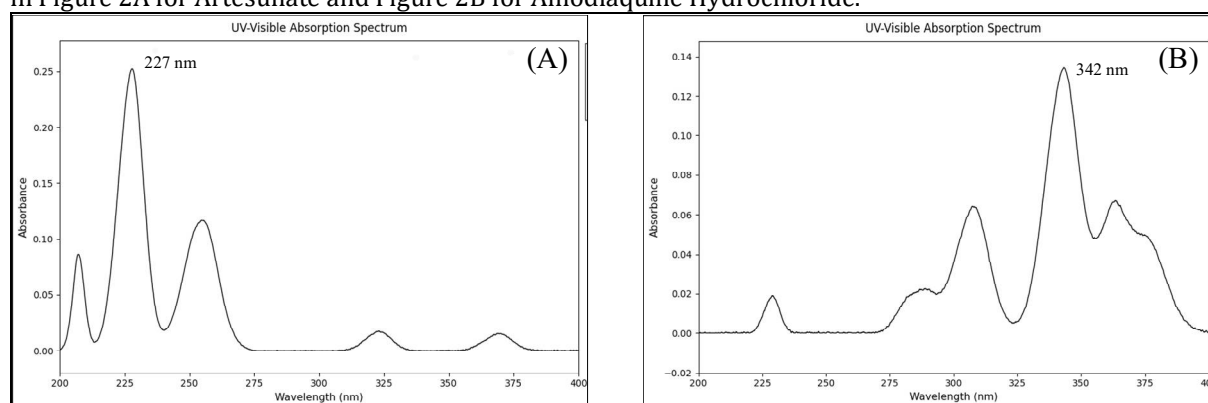


Figure 2: Scanning absorbance maxima of A. Artesunate (227 nm) and B. Amodiaquine

Calibration curve determination

Calibration curves were constructed for both Artesunate and Amodiaquine Hydrochloride using methanolic solutions over a suitable concentration range. Artesunate showed linearity between 5–30 µg/mL with a correlation coefficient (R^2) of 0.9999, while Amodiaquine Hydrochloride showed linearity

between 10–50 µg/mL with an R^2 of 0.9998. The linear regression equations and corresponding graphs are depicted in Figure 3A for Artesunate and Figure 3B for Amodiaquine Hydrochloride.

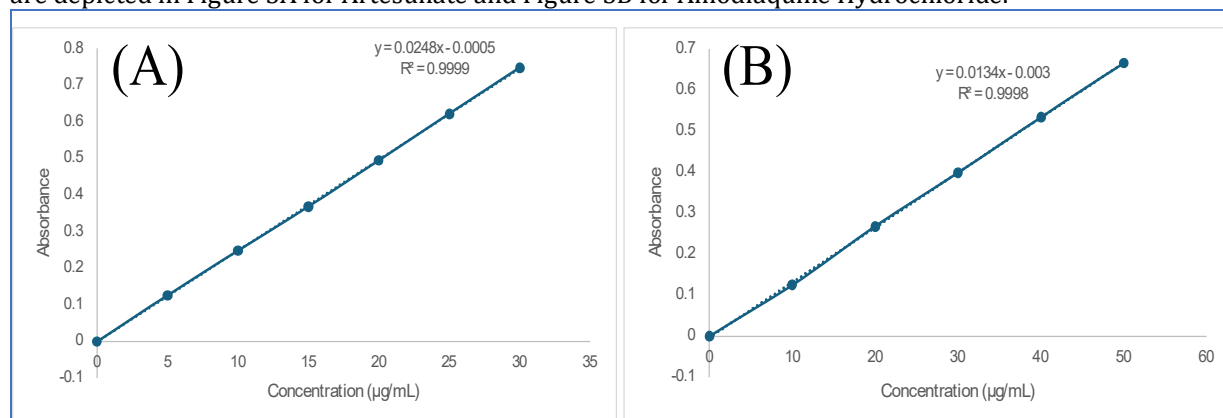


Figure 3: Calibration curve determination of A. Artesunate and B. Amodiaquine in methanol.

Solubility determination in different solvents

The solubility study indicated that artesunate and amodiaquine hydrochloride exhibited minimal solubility in aqueous media, with artesunate showing 0.034 ± 0.002 mg/mL and amodiaquine 0.246 ± 0.006 mg/mL in distilled water. Enhanced solubility was observed in organic solvents, with DMSO and methanol yielding the highest values for both drugs. These findings highlight the need for formulation strategies to improve solubility (Table 4).

Table 4. Solubility of Artesunate and Amodiaquine Hydrochloride in Various Solvents,

Solvent	Solubility of Artesunate (mg/mL)	Category (Artesunate)	Solubility of Amodiaquine Hydrochloride (mg/mL)	Category (Amodiaquine Hydrochloride)
Distilled Water	0.034 ± 0.002	Practically insoluble	0.246 ± 0.006	Slightly soluble
Methanol	5.327 ± 0.084	Slightly soluble	8.641 ± 0.115	Slightly soluble
Ethanol	4.918 ± 0.091	Slightly soluble	7.896 ± 0.102	Slightly soluble
Acetone	3.156 ± 0.073	Slightly soluble	6.874 ± 0.096	Slightly soluble
Dimethyl Sulfoxide (DMSO)	6.843 ± 0.098	Slightly soluble	9.215 ± 0.121	Slightly soluble
Phosphate Buffer (pH 6.8)	0.528 ± 0.012	Very slightly soluble	1.142 ± 0.028	Slightly soluble

All values are expressed as mean \pm SD, n=3.

Differential scanning calorimetry analysis

The differential scanning calorimetry (DSC) analysis demonstrated distinct endothermic peaks for artesunate at 160.25°C and amodiaquine hydrochloride at 149.50°C , confirming their crystalline nature. In the thermogram of the physical mixture, the presence of both characteristic peaks with minimal shift and no new peak formation indicates the absence of any chemical interaction. This suggests good thermal compatibility between the two drugs and the excipients used (Figure 4).

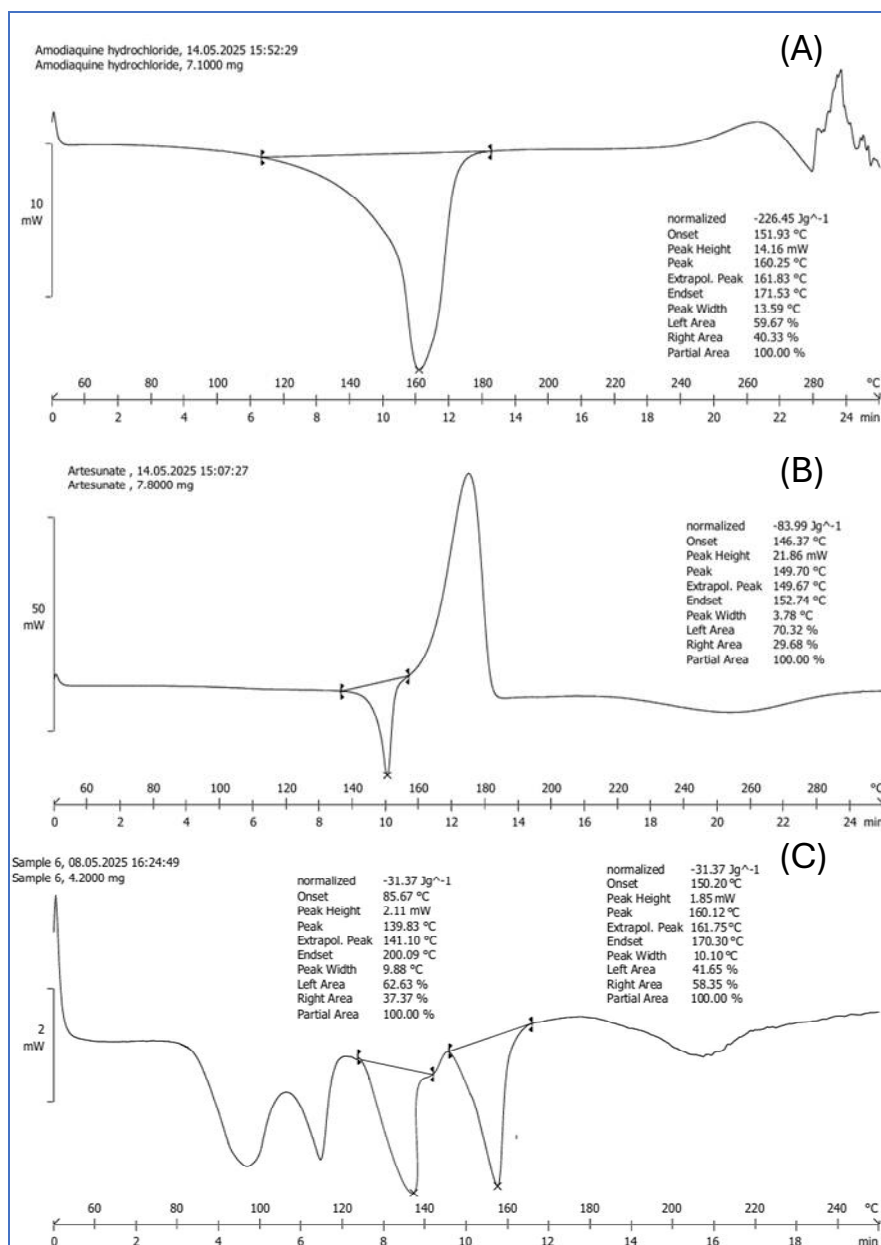


Figure 4: Differential Scanning Calorimetry (DSC) thermograms of (A) Amodiaquine Hydrochloride, (B) Artesunate, and (C) Physical mixture of Amodiaquine Hydrochloride and Artesunate.

FTIR Analysis

FTIR spectral interpretation confirmed the presence of key functional groups in artesunate and amodiaquine hydrochloride, with no significant shifts or disappearance in the physical mixture, indicating compatibility. Notable peaks included the O-H/N-H stretch at $\sim 3300\text{ cm}^{-1}$, C=O stretch at $\sim 1750\text{ cm}^{-1}$, and aromatic ring vibrations around $\sim 1620\text{ cm}^{-1}$. These findings validate the absence of chemical interaction among components (Table 5; Figure 5).

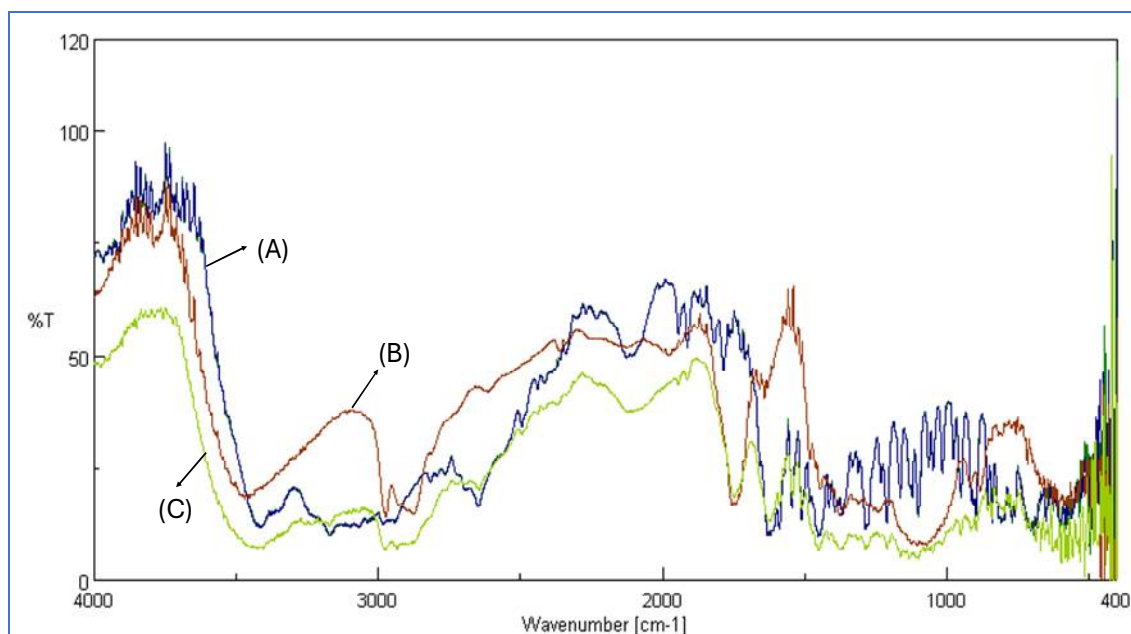


Figure 5: FTIR overlay spectra of (A) Amodiaquine Hydrochloride, (B) Artesunate, and (C) Physical Mixture of Amodiaquine and Artesunate.

Table 5: FTIR Spectral Interpretation of Amodiaquine, Artesunate, and Their Physical Mixture

Sr. No	Standard Wavelength (cm ⁻¹)	Observed in Amodiaquine (cm ⁻¹)	Observed in Artesunate (cm ⁻¹)	Observed in Physical Mixture (cm ⁻¹)
1	3420–3400 (O–H/N–H stretch)	3422.06	3283.21	Overlapping broad peak (~3300)
2	3160–3100 (N–H stretch)	3167.51	–	Present (~3100)
3	2650–2850 (C–H stretch)	2650.68	2866.67	~2850
4	1750–1700 (C=O stretch)	–	1752.98	~1750
5	1660–1620 (C=C or aromatic ring)	1625.70	1664.27	~1620
6	1450–1390 (C–H bending)	–	1397.20	~1400
7	1210–1080 (C–N / C–O stretching)	1216.86, 1085.73	–	~1100–1200
8	880–690 (Aromatic C–H out-of-plane)	693.84	879.41	~700–880
9	2100–2200 (C≡C / C≡N stretch)	2111.67	–	~2100
10	400–500 (Fingerprint region)	485.09	–	~480

Characterization of Dual-Release Inlay Tablets

All batches of the dual-release inlay tablets exhibited consistent organoleptic properties, appearing light yellow in color with a round, biconvex shape and smooth, intact surfaces. No batch showed any visible defects such as cracks or mottling, and all were odorless, indicating uniformity in formulation aesthetics and compliance with standard quality attributes (Table 6).

Table 6: Organoleptic Evaluation of Dual-Release Inlay Tablets

Batch Code	Color	Shape	Surface Appearance	Odor
PF1	Light yellow	Round, biconvex	Smooth, intact	Odorless
PF2	Light yellow	Round, biconvex	Smooth, intact	Odorless
PF3	Light yellow	Round, biconvex	Smooth, intact	Odorless
PF4	Light yellow	Round, biconvex	Smooth, intact	Odorless
PF5	Light yellow	Round, biconvex	Smooth, intact	Odorless
PF6	Light yellow	Round, biconvex	Smooth, intact	Odorless
PF7	Light yellow	Round, biconvex	Smooth, intact	Odorless
PF8	Light yellow	Round, biconvex	Smooth, intact	Odorless
PF9	Light yellow	Round, biconvex	Smooth, intact	Odorless
PF10	Light yellow	Round, biconvex	Smooth, intact	Odorless
PF11	Light yellow	Round, biconvex	Smooth, intact	Odorless
PF12	Light yellow	Round, biconvex	Smooth, intact	Odorless
PF13	Light yellow	Round, biconvex	Smooth, intact	Odorless

The evaluation of physical parameters showed that all batches of dual-release inlay tablets met standard quality specifications. Average tablet weight ranged from 497.5 ± 1.8 mg to 502.3 ± 2.0 mg, indicating uniform die filling. Thickness values were consistent across batches (5.47 ± 0.02 mm to 5.61 ± 0.05 mm), and friability remained well below 1%, confirming mechanical integrity. Hardness values varied between 5.90 ± 0.03 and 6.60 ± 0.04 kg/cm², indicating adequate tablet strength (Table 7).

Table 7: Evaluation of Weight Variation, Thickness, Friability, and Hardness of Dual-Release Inlay Tablets

Batch Code	Avg. Weight (mg)	Thickness (mm)	Friability (%)	Hardness (kg/cm ²)
PF1	498.6 ± 1.9	5.52 ± 0.04	0.28	5.90 ± 0.04
PF2	501.2 ± 2.1	5.56 ± 0.03	0.31	6.15 ± 0.03
PF3	499.7 ± 1.6	5.48 ± 0.02	0.35	6.30 ± 0.05
PF4	500.9 ± 2.3	5.61 ± 0.05	0.27	6.60 ± 0.04
PF5	497.5 ± 1.8	5.50 ± 0.04	0.29	5.96 ± 0.03
PF6	502.3 ± 2.0	5.59 ± 0.03	0.33	5.92 ± 0.05
PF7	500.2 ± 2.4	5.53 ± 0.05	0.26	6.20 ± 0.03
PF8	499.1 ± 1.7	5.49 ± 0.04	0.30	6.54 ± 0.04
PF9	498.9 ± 1.9	5.51 ± 0.03	0.28	6.30 ± 0.03
PF10	500.7 ± 2.2	5.54 ± 0.04	0.34	5.94 ± 0.03
PF11	501.5 ± 1.8	5.60 ± 0.03	0.25	5.94 ± 0.04
PF12	498.3 ± 2.0	5.47 ± 0.02	0.32	5.90 ± 0.03
PF13	499.4 ± 1.6	5.55 ± 0.04	0.29	6.40 ± 0.05

All values are expressed as mean \pm SD

The disintegration time for the immediate-release layer of all dual-release inlay tablet batches ranged from 62 ± 2 to 78 ± 3 seconds, meeting pharmacopeial limits for rapid disintegration. Drug content uniformity was within the acceptable range, with artesunate content between $97.9 \pm 1.0\%$ and $99.4 \pm 1.0\%$, and amodiaquine hydrochloride content ranging from $97.6 \pm 1.3\%$ to $99.3 \pm 1.0\%$, indicating uniform drug distribution across tablets (Table 8).

Table 8: Disintegration Time of Immediate Release Layer and Drug Content Uniformity of Dual-Release Inlay Tablets

Batch Code	Disintegration Time (Sec)	Artesunate Content (%)	Amodiaquine HCl Content (%)
PF1	68 ± 2	98.5 ± 1.1	97.8 ± 1.3
PF2	72 ± 3	99.1 ± 1.2	98.2 ± 1.1
PF3	76 ± 2	97.9 ± 1.0	98.9 ± 1.2
PF4	64 ± 2	98.8 ± 1.3	99.0 ± 1.0
PF5	70 ± 2	98.2 ± 1.4	97.6 ± 1.3
PF6	75 ± 3	99.4 ± 1.0	98.3 ± 1.2
PF7	66 ± 2	98.6 ± 1.2	98.7 ± 1.1
PF8	62 ± 2	99.0 ± 1.1	99.3 ± 1.0
PF9	78 ± 3	98.1 ± 1.3	97.9 ± 1.4
PF10	65 ± 2	98.9 ± 1.0	98.5 ± 1.2
PF11	69 ± 2	98.7 ± 1.2	98.0 ± 1.3
PF12	71 ± 3	98.3 ± 1.1	97.7 ± 1.2
PF13	67 ± 2	99.2 ± 1.0	98.8 ± 1.1

All values are expressed as mean \pm SD

The in-vitro dissolution profile of the immediate-release layer revealed rapid drug release of artesunate, with all batches showing more than 94% release within 30 minutes. Among them, PF8 exhibited the highest release at $97.8 \pm 1.1\%$, demonstrating effective disintegration and dissolution performance (Table 9). For the sustained-release layer, amodiaquine hydrochloride showed a controlled release pattern, with cumulative drug release ranging from $96.02 \pm 0.9\%$ to $99.1 \pm 0.9\%$ at 12 hours. PF4 and PF13 showed the highest release, confirming the efficiency of matrix polymers in sustaining the drug release over the desired period (Table 10).

Table 9: In-vitro Drug Dissolution Profile of Immediate Release Layer (Artesunate)

Time (min)	PF1	PF2	PF3	PF4	PF5	PF6	PF7	PF8	PF9	PF10	PF11	PF12	PF13
0	0.0 ± 0.00	0.0 ± 0.00	0.0 ± 0.00	0.0 ± 0.00	0.0 ± 0.00	0.0 ± 0.00	0.0 ± 0.00	0.0 ± 0.00	0.0 ± 0.00	0.0 ± 0.00	0.0 ± 0.00	0.0 ± 0.00	0.0 ± 0.00
1	9.8 ± 0.7	10.2 ± 0.6	10.9 ± 0.8	11.4 ± 0.7	10.0 ± 0.7	9.5 ± 0.6	10.3 ± 0.8	11.9 ± 0.7	10.7 ± 0.7	10.1 ± 0.8	9.9 ± 0.7	9.6 ± 0.6	10.5 ± 0.7
5	37.4 ± 1.2	38.9 ± 1.3	41.1 ± 1.1	42.5 ± 1.3	39.0 ± 1.2	36.8 ± 1.1	38.7 ± 1.2	43.2 ± 1.4	40.9 ± 1.3	39.5 ± 1.2	38.2 ± 1.1	36.9 ± 1.3	40.3 ± 1.2
10	60.1 ± 1.4	62.3 ± 1.2	65.4 ± 1.3	67.0 ± 1.2	63.1 ± 1.1	59.2 ± 1.3	61.5 ± 1.2	68.5 ± 1.4	65.1 ± 1.3	63.4 ± 1.1	61.0 ± 1.2	59.3 ± 1.3	64.0 ± 1.2
15	75.6 ± 1.3	77.2 ± 1.2	80.1 ± 1.4	81.8 ± 1.3	78.5 ± 1.3	74.0 ± 1.2	76.2 ± 1.3	83.2 ± 1.4	80.3 ± 1.4	78.9 ± 1.3	76.1 ± 1.3	74.5 ± 1.2	79.6 ± 1.3
20	85.2 ± 1.2	86.8 ± 1.3	89.3 ± 1.4	90.6 ± 1.2	87.5 ± 1.1	83.7 ± 1.3	85.1 ± 1.3	91.2 ± 1.4	89.0 ± 1.3	87.1 ± 1.2	85.5 ± 1.2	83.8 ± 1.1	88.4 ± 1.3
25	91.1 ± 1.1	92.0 ± 1.2	93.5 ± 1.1	94.4 ± 1.2	92.7 ± 1.1	90.1 ± 1.2	91.0 ± 1.2	95.0 ± 1.3	93.3 ± 1.2	92.0 ± 1.2	91.4 ± 1.2	90.0 ± 1.1	93.1 ± 1.2
30	94.9 ± 1.0	95.7 ± 1.1	96.6 ± 1.1	97.2 ± 1.1	96.0 ± 1.0	94.2 ± 1.1	95.1 ± 1.0	97.8 ± 1.1	96.4 ± 1.1	95.8 ± 1.1	95.0 ± 1.1	94.0 ± 1.0	96.5 ± 1.1

All values are expressed as mean ± SD, n=3.

Table 10: In-vitro Drug Dissolution Profile of Sustained-Release Layer (Amodiaquine HCl)

Time (h)	PF1	PF2	PF3	PF4	PF5	PF6	PF7	PF8	PF9	PF10	PF11	PF12	PF13
0	0.00 ± 0.00	0.00 ± 0.00	0.00 ± 0.00	0.00 ± 0.00	0.00 ± 0.00	0.00 ± 0.00	0.00 ± 0.00	0.00 ± 0.00	0.00 ± 0.00	0.00 ± 0.00	0.00 ± 0.00	0.00 ± 0.00	0.00 ± 0.00
1	14.2 ± 0.5	13.5 ± 0.4	15.1 ± 0.6	12.9 ± 0.5	14.0 ± 0.4	13.8 ± 0.5	12.7 ± 0.6	15.5 ± 0.5	14.7 ± 0.6	13.3 ± 0.5	14.1 ± 0.5	13.9 ± 0.4	14.3 ± 0.5
2	26.8 ± 0.6	25.9 ± 0.5	28.2 ± 0.6	24.4 ± 0.7	27.0 ± 0.6	26.5 ± 0.6	24.1 ± 0.6	28.7 ± 0.7	27.3 ± 0.6	25.2 ± 0.5	26.6 ± 0.6	26.2 ± 0.6	27.1 ± 0.5
4	44.5 ± 0.7	43.0 ± 0.8	46.8 ± 0.7	40.3 ± 0.6	45.2 ± 0.7	44.0 ± 0.8	39.5 ± 0.6	47.5 ± 0.7	46.0 ± 0.7	42.5 ± 0.6	44.6 ± 0.8	43.8 ± 0.7	45.3 ± 0.6
6	62.7 ± 0.8	60.4 ± 0.7	65.1 ± 0.8	56.2 ± 0.7	63.8 ± 0.8	61.9 ± 0.9	54.7 ± 0.7	66.0 ± 0.8	64.2 ± 0.7	59.7 ± 0.7	62.5 ± 0.8	61.0 ± 0.8	63.6 ± 0.7
8	78.9 ± 0.9	76.8 ± 0.8	81.5 ± 0.8	70.3 ± 0.9	80.1 ± 0.8	78.2 ± 0.9	68.7 ± 0.9	82.0 ± 0.9	80.5 ± 0.9	75.4 ± 0.9	78.6 ± 0.8	76.9 ± 0.9	79.3 ± 0.8
10	89.6 ± 0.8	87.2 ± 0.7	91.7 ± 0.9	83.4 ± 0.8	90.5 ± 0.9	88.3 ± 0.8	81.0 ± 0.9	92.2 ± 0.8	90.8 ± 0.9	86.3 ± 0.9	88.9 ± 0.9	87.1 ± 0.8	89.7 ± 0.8
12	96.1 ± 0.9	96.89 ± 0.8	98.06 ± 0.9	99.1 ± 0.9	96.07 ± 0.8	96.02 ± 0.9	97.05 ± 0.8	98.9 ± 0.9	98.0 ± 0.9	96.4 ± 0.8	96.1 ± 0.8	96.04 ± 0.9	99.1 ± 0.9

All values are expressed as mean ± SD, n=3.

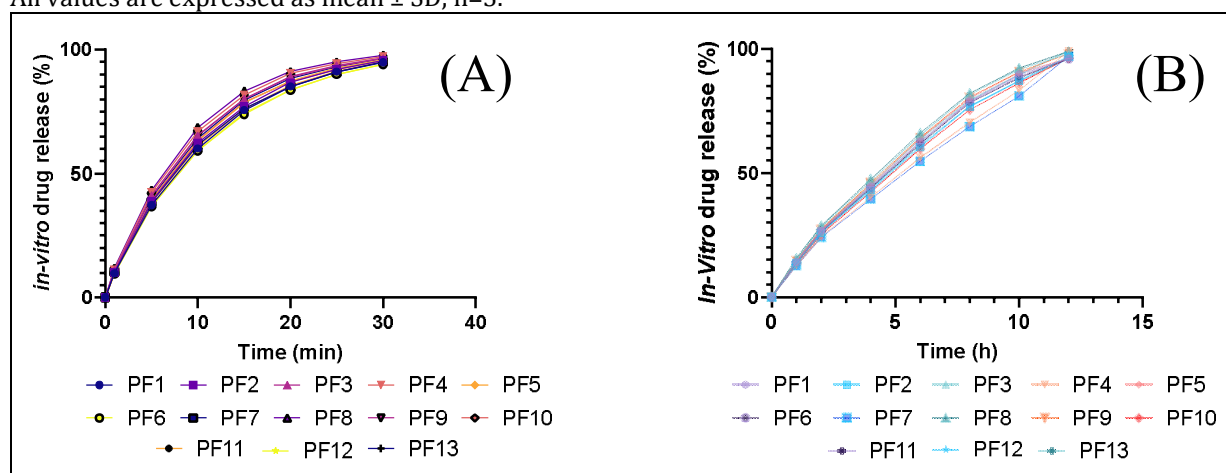


Figure 6: In-vitro Drug Dissolution Profiles of Dual-Release Inlay Tablet: (A) Immediate Release Layer Containing Artesunate and (B) Sustained Release Layer Containing Amodiaquine Hydrochloride.

Optimization

In-vitro Drug Dissolution at 12 Hr

The statistical modeling for in-vitro drug dissolution at 12 hr confirmed the suitability of a quadratic model, as evidenced by a highly significant sequential p-value of 5.36×10^{-8} and non-significant lack of fit ($p = 0.6277$) (Table 11). The model exhibited excellent predictive reliability, with an adjusted R^2 of 0.9884 and a predicted R^2 of 0.9772, indicating strong internal consistency. ANOVA analysis (Table 12) revealed the model was statistically significant ($F = 205.13$, $p = 1.97 \times 10^{-7}$), with HPMC K4M (B) exerting a major linear effect ($F = 124.17$, $p = 1.04 \times 10^{-5}$), followed by significant contributions from the interaction term AB ($F = 71.08$, $p = 6.51 \times 10^{-5}$) and the quadratic terms A^2 ($F = 820.60$, $p = 1.62 \times 10^{-8}$) and B^2 ($F = 44.93$, $p = 0.0003$). In contrast, Ethyl cellulose (A) was not significant ($p = 0.3849$).

The polynomial regression equation derived for drug release at 12 hr was:

$$Y_1 = 96.142 + 0.0441053 * A + 0.53038 * B + -0.5675 * AB + 1.46213 * A^2 + 0.342125 * B^2$$

The coefficients indicate a prominent influence of the quadratic term A^2 (2.53), followed by positive contributions from both HPMC K4M ($B = 1.35$) and the interaction term AB (1.14). The 2D contour and 3D surface plots (Figure 7A–7B) visually confirmed this trend, showing maximum drug release in the mid to high ranges of B while maintaining moderate levels of A. The pronounced curvature in the response surface indicates a strong non-linear relationship, particularly along the B-axis, signifying that higher levels of HPMC K4M enhance release efficiency, especially in the presence of Ethyl cellulose.

Tablet Hardness

The quadratic model selected for tablet hardness demonstrated high statistical adequacy, confirmed by a sequential p-value of 1.13×10^{-7} and an acceptable lack of fit p-value of 0.2559, as shown in Table 11. The model fit statistics were strong, with an adjusted R^2 of 0.9839 and a predicted R^2 of 0.9539, reflecting high correlation between observed and predicted values. According to ANOVA results (Table 12), the model was highly significant ($F = 147.38$, $p = 6.20 \times 10^{-7}$), and the primary contributors were HPMC K4M (B) ($F = 50.66$, $p = 0.0002$), interaction term AB ($F = 15.17$, $p = 0.0059$), and the quadratic terms A^2 ($F = 666.61$, $p = 3.34 \times 10^{-8}$) and B^2 ($F = 23.62$, $p = 0.0018$). Ethyl cellulose (A) was not a statistically significant factor ($p = 0.1809$).

The polynomial regression equation for tablet hardness is:

$$Y_2 = 5.928 + 0.0168566 * A + 0.0807475 * B + -0.0625 * AB + 0.314125 * A^2 + 0.059125 * B^2$$

The equation shows a dominant quadratic influence of A^2 (0.52) and B^2 (0.21) on hardness, while the main effects of A and B were moderate. The corresponding contour and response surface plots (Figure 7C–7D) support these findings, illustrating increased hardness values in the region of high Ethyl cellulose concentration and moderate HPMC K4M levels. The curvature pattern indicates a synergistic influence of both polymers, with peak hardness obtained at higher A levels, although excessive B resulted in plateauing effects. These visual trends align closely with the polynomial model, confirming the importance of curvature and interaction in optimizing mechanical strength.

Table 11: Model Fit Summary for Response Variables of Dual-Release Tablet Formulation

Response Variable	Model	Sequential p-value	Lack of Fit p-value	Adjusted R^2	Predicted R^2
In-vitro Drug Dissolution at 12 hr	Quadratic	< 0.0001	0.6277	0.9884	0.9772
Tablet Hardness	Quadratic	< 0.0001	0.2559	0.9839	0.9539

Table 12: ANOVA Results for Quadratic Models of Response Variables

Source	Sum of Squares	df	Mean Square	F-value	p-value	Significance
In-vitro Drug Dissolution (12 hr)						
Model	18.59	5	3.7176	205.13	< 0.0001	significant
A – Ethyl cellulose	0.0156	1	0.0156	0.859	< 0.0001	significant
B – HPMC K4M	2.25	1	2.2504	124.17	< 0.0001	significant
AB	1.29	1	1.2882	71.08	< 0.0001	significant
A^2	14.87	1	14.8717	820.60	< 0.0001	significant
B^2	0.8143	1	0.8143	44.93	0.0003	significant
Tablet Hardness						
Model	0.7588	5	0.1518	147.38	< 0.0001	significant
A – Ethyl cellulose	0.0023	1	0.0023	2.21	0.1809	Not significant
B – HPMC K4M	0.0522	1	0.0522	50.66	0.0002	significant
AB	0.0156	1	0.0156	15.17	0.0059	significant
A^2	0.6864	1	0.6864	666.61	< 0.0001	significant
B^2	0.0243	1	0.0243	23.62	0.0018	significant

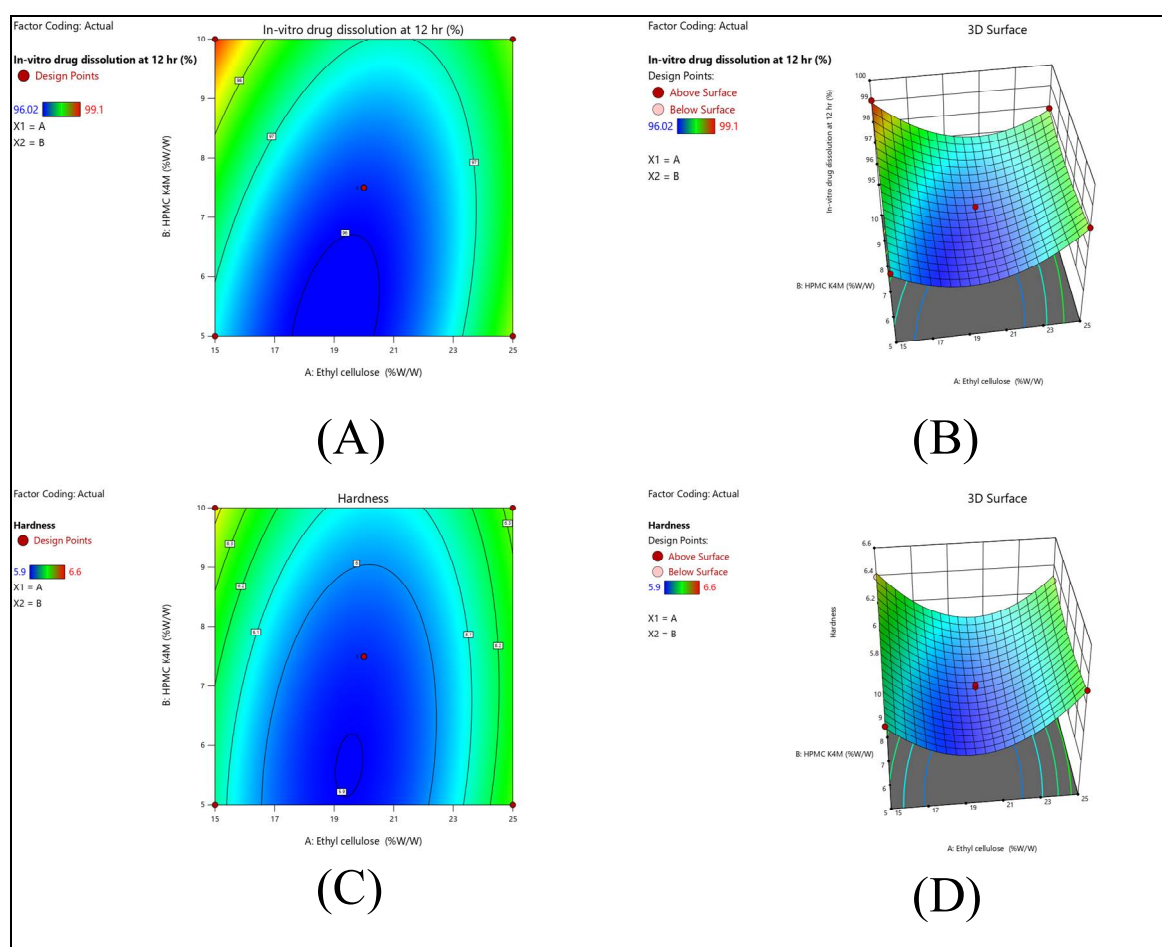


Figure 7: Two-dimensional contour plots and corresponding three-dimensional surface response plots illustrating the effect of Ethyl cellulose (X_1) and HPMC K4M (X_2) concentrations on (A–B) in-vitro drug dissolution at 12 hr and (C–D) tablet hardness. The plots depict the interaction and curvature effects of formulation variables on the selected responses within the design space.

Statistical optimization of formulation

Statistical optimization using the Central Composite Design identified PF8 as the optimized formulation based on the desirability function. It comprised 12.92% ethyl cellulose and 7.5% HPMC K4M. The predicted in-vitro drug dissolution at 12 hours was 99.00%, closely matching the experimental value of 98.9%, with a relative error of just 0.10%. Similarly, the predicted hardness was 6.428 kg/cm² compared to the experimental value of 6.54 kg/cm², indicating a minimal deviation of 1.74% (Table 13).

Table 13: Statistical optimization of formulation

F. Code	Composition	Amount (% w/w)	Response	Predicted Value	Experimental Value	Relative Error (%)
PF8	Ethyl cellulose	12.92	In-vitro Drug Dissolution at 12 hr (%)	99.00	98.9	0.10
	HPMC K4M	7.5	Hardness (kg/cm ²)	6.428	6.54	1.74

Release kinetics

The release kinetics study demonstrated that the immediate-release layer containing artesunate followed first-order kinetics, indicated by a high correlation coefficient ($R^2 = 0.9979$), signifying concentration-dependent drug release. In contrast, the sustained-release layer of amodiaquine hydrochloride best fit the Hixson–Crowell model, with an R^2 value of 0.9827, suggesting that drug release was influenced by changes in surface area and tablet geometry during dissolution (Figure 8).

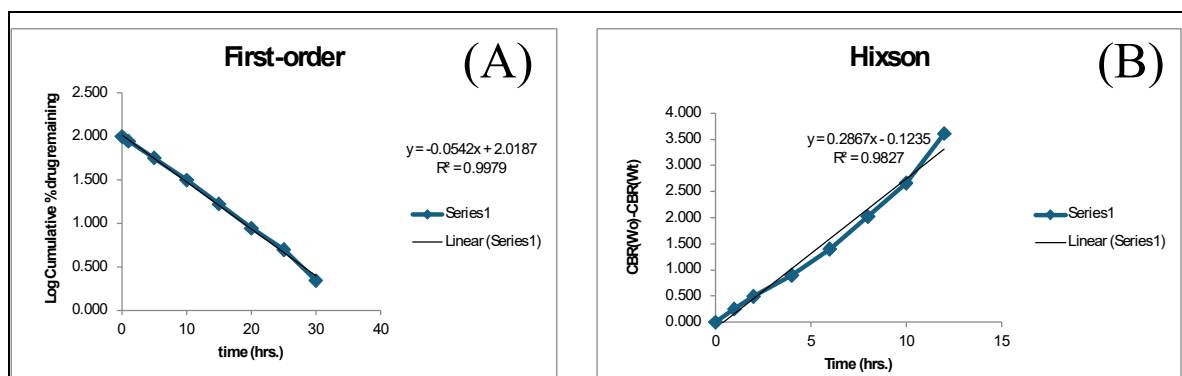


Figure 8: Drug Release Kinetics of Dual-Release Inlay Tablet: (A) First-Order Kinetic Plot for Immediate Release Layer (Artesunate), (B) Hixson-Crowell Model Plot for Sustained Release Layer (Amodiaquine Hydrochloride).

***In-vitro* cell cytotoxicity study**

The in-vitro cytotoxicity study using the MTT assay on THP-1 cells revealed a dose-dependent decrease in cell viability upon exposure to increasing concentrations of the dual-release inlay tablet. At 500 µg/mL, cell survival was reduced to $42.88 \pm 3.08\%$, with an IC_{50} value calculated as 114.61 µg/mL. These results confirm moderate cytotoxic activity and support the safe therapeutic window of the formulation (Table 14; Figures 9 and 10).

Table 14: In-vitro Cytotoxicity Profile of Dual-Release Inlay Tablet in THP-1 Cells (MTT Assay)

Concentration (µg/mL)	% Cell Survival \pm SD
0 (Control)	100.00 \pm 3.79
1	71.65 \pm 2.62
5	61.06 \pm 1.65
25	53.28 \pm 4.75
50	54.70 \pm 4.53
100	50.27 \pm 5.75
250	51.85 \pm 2.45
500	42.88 \pm 3.08
IC_{50} Value	114.61 µg/mL

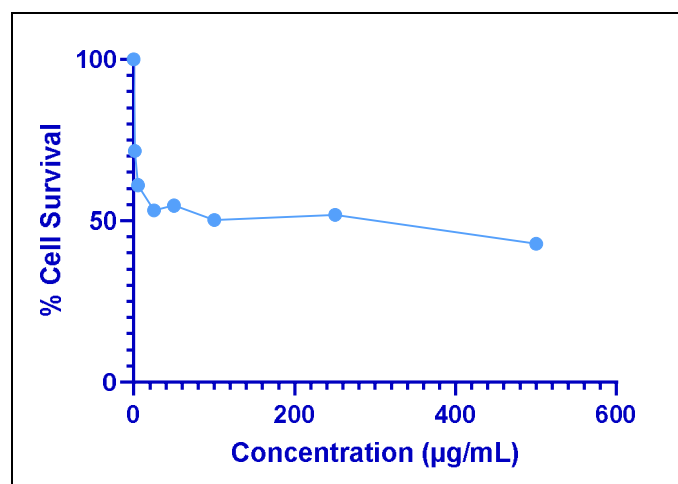


Figure 9: In-vitro cytotoxicity of formulation against THP-1

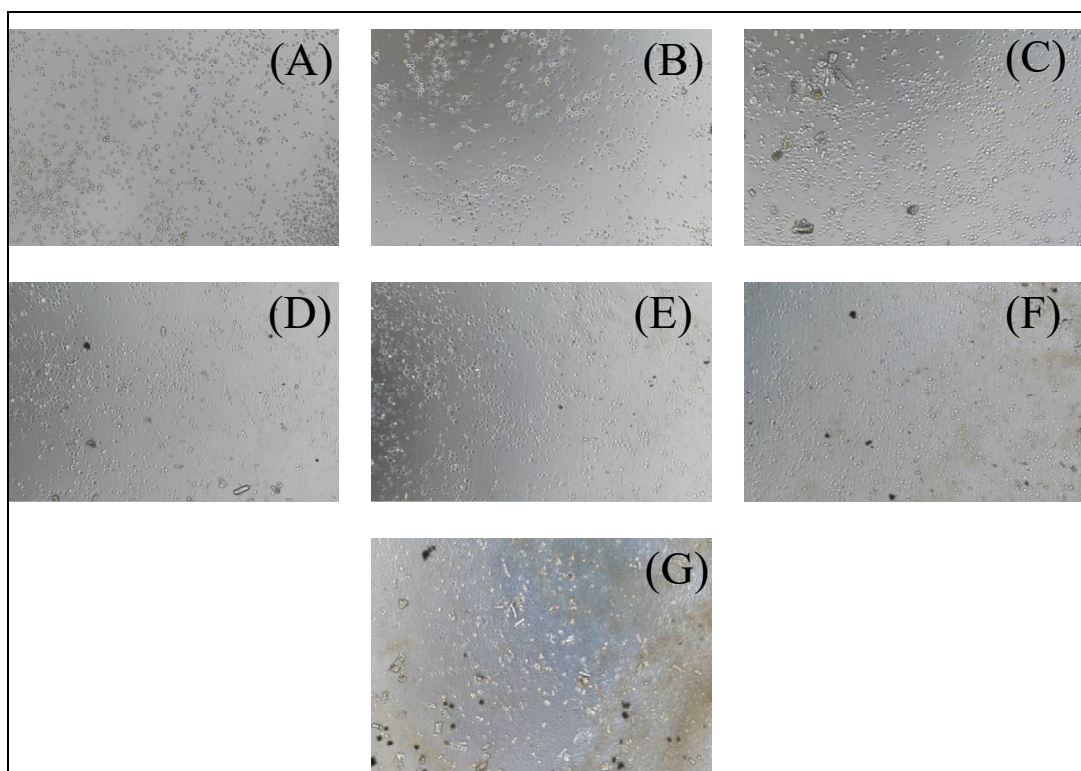


Figure 10: Microscopic images showing morphological changes in THP-1 cells after 24-hour exposure to increasing concentrations of Artesunate. (A) Control (0 µg/mL), (B) 1 µg/mL, (C) 5 µg/mL, (D) 25 µg/mL, (E) 50 µg/mL, (F) 100 µg/mL, and (G) 500 µg/mL.

Stability study

The stability study of the optimized formulation PF8 under accelerated conditions ($40 \pm 2^\circ\text{C}$, $75 \pm 5\%$ RH) over three months showed no significant changes in physical appearance, hardness, friability, drug content, disintegration time, or drug release. Artesunate and amodiaquine HCl content remained above 98%, and drug release at respective time points remained consistent, indicating that the formulation maintained its integrity and performance throughout the study period (Table 15).

Table 15: Stability Study of Optimized Batch PF8

Parameter	Initial (0 Month)	1 Month	2 Months	3 Months
Physical Appearance	Intact, light yellow	No change	No change	No change
Hardness (kg/cm^2)	6.54 ± 0.04	6.52 ± 0.03	6.50 ± 0.05	6.48 ± 0.04
Friability (%)	0.30	0.31	0.32	0.33
Artesunate Content (%)	99.0 ± 1.1	98.7 ± 1.0	98.5 ± 1.1	98.2 ± 1.0
Amodiaquine HCl Content (%)	99.3 ± 1.0	98.9 ± 1.1	98.6 ± 1.2	98.4 ± 1.0
Disintegration Time (Sec)	62 ± 2	63 ± 2	64 ± 2	65 ± 2
Artesunate Release (30 min, %)	97.8 ± 1.1	97.5 ± 1.0	97.2 ± 1.2	97.0 ± 1.1
Amodiaquine Release (12 hr, %)	98.9 ± 0.9	98.6 ± 1.0	98.2 ± 0.8	97.9 ± 0.9

All values are expressed as mean \pm SD (n=3).

DISCUSSION

Developing and optimizing the dual-release formulation with artesunate as the immediate layer and amodiaquine hydrochloride in the long-acting core helped match how effective the drug is at different stages of treatment. Artesunate was detected at 227 nm and amodiaquine hydrochloride at 342 nm which made reliable wavelength selection for the next analyses possible (Figure 2). The calibration graphs in methanol showed high linearity, with r^2 values of 0.9999 for artesunate and 0.9998 for amodiaquine, demonstrating that the analysis was accurate and precise (as seen in Figure 3) [44]. It was demonstrated that no matter how much water was used, the solubility of artesunate was nearly zero and that of amodiaquine hydrochloride was very low. On the other hand, the drugs dissolved much better in organic solvents like methanol and DMSO (Table 4). Based on the findings, it is very important to create a formulation that will improve solubility and help release both drugs, paying particular attention to amodiaquine hydrochloride as the main drug staying in the pills for a long period [38].

Excipient compatibility with the drugs was proven using DSC and FTIR methods. Artesunate and amodiaquine hydrochloride thermograms demonstrated clearly marked endothermic peaks at 160.25°C and 149.50°C, respectively. These peaks were unchanged in the mix and no new peaks appeared which proves no interaction and thermal compatibility for the drugs (Figure 4). In the same manner, the physical mixture showed all significant peaks of the drugs, for instance, the O–H/N–H and C=O stretches of both drugs, as seen by the FTIR spectra (Table 5; Figure 5). Tablet characteristics were consistent across all the 13 tested formulations. Each group of tablets had a light yellow color, round shape, a smooth surface and no odor which made them meet the requirements in terms of appearance and sense (Table 6) [39]. All physical parameters were within the range indicated in the pharmacopeia, showing that the formulation is robust and mechanically stable (Table 7). Over 62 to 78 seconds, the immediate-release layer disintegrated and allowed artesunate to be quickly released. All the doses had acceptable amounts of both artesunate and amodiaquine which were within the range of 97.9% to 99.4% for artesunate and 97.6% to 99.3% for amodiaquine (Table 8). The chart shows that the immediate-release layer allows for swift release of artesunate, with every batch releasing >94% in just 30 minutes and PF8 achieving even more at $97.8 \pm 1.1\%$ (Table 9). The controlled release level of amodiaquine hydrochloride was found to be steady and it ranged from 96.02% to 99.1% of cumulative release over 12 hours, indicating that the matrix was modified successfully (Table 10; Figure 6) [40,41].

The use of Central Composite Design in statistics proved that quadratic models are adequate for explaining both drug release and the hardness of tablets. It was found in ANOVA that K4M HPMC had a significant positive effect on drug release and hardness and that ethyl cellulose increased hardness in a quadratic manner, mainly affecting the hardness of formulated tablets (Tables 11 and 12). For the PF8 formulation, consisting of 12.92% ethyl cellulose and 7.5% HPMC K4M, both the predicted and the experimental results for drug release (99.00% and 98.9%, respectively) and the hardness (6.428 kg/cm^2 and 6.54 kg/cm^2) were in good agreement, with minimal errors of 0.10% and 1.74% (Table 13; Figure 7) [42]. Results of kinetic modeling showed that the artesunate layer was going through a concentration-dependent mechanism, whereas the amodiaquine hydrochloride stream showed signs of a pattern controlled by the shape of the tablet ($R^2 = 0.9979$ and $R^2 = 0.9827$ respectively). They show that the release in the dual-layered system is adapted for carrying out combination therapy. Dose-dependent cell death was observed and THP-1 cells survived at $500 \mu\text{g/mL}$ with only $42.88 \pm 3.08\%$ viability [43]. The data indicate that these compounds have modest cytotoxic effects which makes them potentially safe to use in the mouth (Table 14; Figures 9 and 10). The changes seen with a microscope confirmed that the cells were damaged at higher levels of estrogen exposure. Three-month tests carried out on PF8 following ICH guidance found that the drug did not change in physical form, drug potency or how it was released. The percentage of artesunate and amodiaquine did not go below 98% and the drug release at given times stayed unchanged from the initial values, showing that the combination was chemically and physically stable (see Table 15) [44].

CONCLUSION

Throughout the study, a dual-release tablet was successfully created and fine-tuned, with artesunate for fast-acting release and amodiaquine hydrochloride for a more extended effect, to try to enhance match sequential drug doses in treating malaria and improve compliance. This final formulation (PF8) was found to have strong physical functions, was gradual in releasing the drug in lab conditions and showed compatibility and stability. The pattern of drug release from each layer was nicely fitted by first-order and Hixson–Crowell models. Studies measuring cytotoxicity found that the product is safe enough for use. According to this, maintaining both drugs in the body could increase treatment success, as it needs fewer doses and is likely to be more followed by patients. More experiments in animals are advised to assure the drug level and its effect, showing that this formulation is suitable for use in antimalarial treatment.

Abbreviations

ANOVA: Analysis of Variance; FTIR: Fourier-transform Infrared Spectroscopy; UV: Ultra-violet Spectroscopy; Df: Degree of Freedom; DSC: Differential Scanning Calorimetry; SD: Standard Deviation; MTT: 3-(4,5-Dimethylthiazol-2-yl)-2,5-diphenyltetrazolium bromide; IC_{50} : Half-maximal Inhibitory Concentration; HPMC: Hydroxypropyl Methylcellulose; RH: Relative Humidity; PF: Prototype Formulation; THP-1: Human Monocytic Cell Line; R^2 : Coefficient of Determination.

ACKNOWLEDGEMENT

The authors deeply thank Dr. Vithalrao Vikhe Patil Foundation's College of Pharmacy in Ahmednagar for enabling this research through their necessary facilities. At the conclusion we thank the members of the

Department of Pharmaceutical Quality Assurance who continuously supported us with their guidance during every step of this work.

Authors contribution

All authors contributed equally.

Conflict of interest

The authors declare no conflict of interest.

Funding

Nil

REFERENCES

1. Shin H-I, Ku B, Park E, Ju J-W, Lee H-I. (2021) Status of World Malaria in (2022 World Malaria Report) 2023;16:684–706.
2. Shin H-I, Ku B, Jung H, Lee S, Lee S-Y, Ju J-W, et al. (2023). World Malaria Report (Status of World Malaria in 2022) 2024; 17:1351–77.
3. Andrade MV, Noronha K, Diniz BPC, Guedes G, Carvalho LR, Silva VA, et al. (2022). The economic burden of malaria: a systematic review. *Malar J*; 21:283.
4. Kulkarni MA, Duguay C, Ost K. (2022). Charting the evidence for climate change impacts on the global spread of malaria and dengue and adaptive responses: a scoping review of reviews. *Global Health*; 18:1.
5. Kendie FA, Hailegebriel W/kiros T, Nibret Semegn E, Ferede MW. (2021). Prevalence of Malaria among Adults in Ethiopia: A Systematic Review and Meta-Analysis. *Journal of Tropical Medicine*; 2021:8863002.
6. Ruwizhi N, Maseko RB, Aderibigbe BA. (2022). Recent Advances in the Therapeutic Efficacy of Artesunate. *Pharmaceutics*; 14:504.
7. Pawłowska M, Mila-Kierzenkowska C, Szczegielniak J, Woźniak A. 2024 (). Oxidative Stress in Parasitic Diseases—Reactive Oxygen Species as Mediators of Interactions between the Host and the Parasites. *Antioxidants*; 13:38.
8. Grace OO. (2023). Effects Of Some Anti-Malaria Drugs (Chloroquine, Artesunate and Dihydroartemisinin) On Some Hematological Parameters. *ScienceOpen Preprints*. 10.14293/S2199-1006.1.SOR-PP0ZGYL.v1
9. Marri S. (2024). The Development and Validation of the HPLC Method for Determination of Artesunate and Amodiaquine in Novel Antimalarial Formulations.
10. Abba N, Almond LM, Bonner JJ, Richardson N, Wells TNC, Möhrle JJ. (2024). PBPK-led assessment of antimalarial drugs as candidates for Covid-19: Simulating concentrations at the site of action to inform repurposing strategies. *Clinical and Translational Science*; 17: e13865.
11. Oldfield LR, Mentrup AFC, Klinken-Uth S, Auel T, Seidlitz A. (2024). From design to 3D printing: A proof-of-concept study for multiple unit particle systems (MUPS) printed by dual extrusion fused filament fabrication. *International Journal of Pharmaceutics*; X; 8:100299.
12. Dhanorkar V, Shah P. (2021). Development and characterization of multiparticulate system as an alternative to unit dosage forms containing drugs with diverse release profiles. *Futur J Pharm Sci*; 7:225.
13. Zhang Y, Thakkar R, Zhang J, Lu A, Duggal I, Pillai A, et al. (2023). Investigating the Use of Magnetic Nanoparticles as Alternative Sintering Agents in Selective Laser Sintering (SLS) 3D Printing of Oral Tablets. *ACS Biomater Sci Eng*; 9:2924–36.
14. Yasin H, Al-Tabakha MMA, Chan SY. (2024). Fabrication of Polypill Pharmaceutical Dosage Forms Using Fused Deposition Modeling 3D Printing: A Systematic Review. *Pharmaceutics*; 16:1285.
15. Pavazhaviji P, Rajalakshmi AN. (2022). Fixed-Dose Combination drugs as Tablet in Tablet: A review. *International Journal of Pharmacy Research & Technology (IJPR)*; 12:39–45.
16. El-Naggar NE-A, Shiha AM, Mahrous H, Mohammed ABA. (2022). Green synthesis of chitosan nanoparticles, optimization, characterization and antibacterial efficacy against multi drug resistant biofilm-forming *Acinetobacter baumannii*. *Sci Rep*; 12:19869.
17. Elugoke SE, Fayemi OE, Adekunle AS, Mamba BB, Nkambule TTI, Ebenso EE. (2022). Electrochemical sensor for the detection of dopamine using carbon quantum dots/copper oxide nanocomposite modified electrode. *FlatChem*; 33:100372.
18. Ali MS, Elsaman T. (2021). Development and Validation of the UV Spectrophotometric Method for Simultaneous Determination of Paracetamol and Pseudoephedrine in Bulk and Combined Tablet Dosage Form. *Pharm Chem J*; 54:1306–10.
19. Abu Shawish HM, Saadeh SM, Al-kahlout ST. (2022). PVC membrane, coated-wire, and carbon-paste electrodes for potentiometric determination of vardenafil hydrochloride in tablet formulations and urine samples. *Sensors International*; 3:100175.
20. Shakeel F, Haq N, Alsarra IA. (2021). Equilibrium solubility determination, Hansen solubility parameters and solution thermodynamics of cabozantinib malate in different monosolvents of pharmaceutical importance. *Journal of Molecular Liquids*; 324:115146.

21. Cong Y, Du C, Xing K, Bian Y, Li X, Wang M. (2022). Investigation on co-solvency, solvent effect, Hansen solubility parameter and preferential solvation of fenbufen dissolution and models correlation. *Journal of Molecular Liquids*; 348:118415.
22. Rojek B, Wesolowski M. (2023). A combined differential scanning calorimetry and thermogravimetry approach for the effective assessment of drug substance-exipient compatibility. *J Therm Anal Calorim*; 148:845–58.
23. Brusač E, Jeličić M-L, Cvetnić M, Amidžić Klarić D, Nigović B, Mornar A. (2021). A Comprehensive Approach to Compatibility Testing Using Chromatographic, Thermal and Spectroscopic Techniques: Evaluation of Potential for a Monolayer Fixed-Dose Combination of 6-Mercaptopurine and Folic Acid. *Pharmaceutics*; 14:274.
24. Bunaciu AA, Hoang, Vu Dang, and Aboul-Enein HY. (2025). Fourier transform infrared spectroscopy used in drug excipients compatibility studies. *Applied Spectroscopy Reviews*; 60:385–403.
25. Murillo-Fernández MA, Montero-Zeledón E, Abdala-Saiz A, Vega-Baudrit JR, Araya-Sibaja AM. (2022). Interaction and Compatibility Studies in the Development of Olmesartan Medoxomil and Hydrochlorothiazide Formulations under a Real Manufacturing Process. *Pharmaceutics*; 14:424.
26. Jadhav S, Dighe P, Kumbhare M. (2025). Synthesis In Vitro Evaluation and Molecular Docking Studies of Novel Pyrazoline Derivatives as Promising Bioactive Molecules. *J Pharm Sci Comput Chem*; 1. *J. Pharm. Sci. Comput. Chem.* 2025, 1 [3], 190-209.
27. Gadad AP, Naik SS, Dandagi PM, Baburao U. (2016). Formulation and Evaluation of Gastroretentive Floating Microspheres of Lafutidine n.d. *Indian Journal of Pharmaceutical Education and Research | Vol 50 | Issue 2 (Suppl.)* :76-81
28. Sr M, Bk N, Ab S, T S. (2018). Development and Evaluation of Dual Release Tablet of Metformin and Pioglitazone for the Treatment of Diabetes Mellitus. *Pharm Anal Acta*; 09.
29. Savjani K, Gajjar A, Savjani J. (2016). Modified formulation of febuxostat: improved efficacy and safety. *Int J Pharm Pharm Sci*; 8:359–66.
30. Gandhi K, Shah SK, Tyagi CK, Budholiya P, Pandey H. (2020). Formulation, Development and Evaluation of Uncoated Bilayer Tablet of Anti-Hypertensive Agents. *J Drug Delivery Ther*; 10:100–7.
31. Patel DM, Trivedi R, Patel H. (2021). Formulation and Evaluation of Bi-Layer Tablets of Ketorolac Tromethamine. *J Drug Delivery Ther*; 11:36–41.
32. Singh N, Pandey D, Jain N, Jain S. (2021). Formulation and In Vitro Evaluation of Bilayer Tablets of Lansoprazole and Amoxycillin Trihydrate for the Treatment of Peptic Ulcer. *EBSCOhost*; 11:23.
33. Prohit P, Pakhare P, Pawar V, Dandade S, Waghmare M, Shaikh F, et al. (2025). Formulation and Comparative Evaluation of Naproxen-Based Transdermal Gels. *J Pharm Sci Comput Chem*; 1.
34. Ameen MSM, Ibrahim NJ, Omar TA. (2023). Design and Evaluation of Sustained Release Bilayer Tablets of Oxcarbazepine. *J Pharm Innov*; 18:1213–28.
35. Mubeen I, Zaman M, Farooq M, Mehmood A, Azeez FK, Rehman W, et al. (2022). Formulation of Modified-Release Bilayer Tablets of Atorvastatin and Ezetimibe: An In-Vitro and In-Vivo Analysis. *Polymers*; 14:3770.
36. Lakshani N, Wijerathne HS, Sandaruwan C, Kottegoda N, Karunarathne V. (2023). Release Kinetic Models and Release Mechanisms of Controlled-Release and Slow-Release Fertilizers. *ACS Agric Sci Technol*; 3:939–56.
37. Ali MA, Musthafa SA, Munuswamy-Ramanujam G, Jaisankar V. (2022). 3-Formylindole-based chitosan Schiff base polymer: Antioxidant and *in vitro* cytotoxicity studies on THP-1 cells. *Carbohydrate Polymers*; 290:119501.
38. Mirata S, Almonti V, Di Giuseppe D, Fornasini L, Raneri S, Vernazza S, et al. (2022). The Acute Toxicity of Mineral Fibres: A Systematic In Vitro Study Using Different THP-1 Macrophage Phenotypes. *International Journal of Molecular Sciences*; 23:2840.
39. González-González O, Ramirez IO, Ramirez BI, O'Connell P, Ballesteros MP, Torrado JJ, et al. (2022). Drug Stability: ICH versus Accelerated Predictive Stability Studies. *Pharmaceutics*; 14:2324.
40. Le Berre M, Gerlach JQ, Dziembala I, Kilcoyne M. (2022). Calculating Half Maximal Inhibitory Concentration (IC50) Values from Glycomics Microarray Data Using GraphPad Prism. In: Kilcoyne M, Gerlach JQ, editors. *Glycan Microarrays: Methods and Protocols*, New York, NY: Springer US; p. 89–111.
41. Bhattacharyya HRKAS. (2021). Statistical Optimization and Evaluation of a Multi release Unit Bilayer Tablet of Rizatriptan Benzoate. *Ijps*; 83.
42. Aleti R, Baratam SR, Jagirapu B, Kudamala S. (2021). Formulation And Evaluation Of Metformin Hydrochloride and Gliclazide Sustained Release Bilayer Tablets: A Combination Therapy In Management Of Diabetes. *Int J App Pharm*; 343–50.
43. Lin W, Li Y, Shi Q, Liao X, Zeng Y, Tian W, et al. (2022). Preparation and evaluation of bilayer-core osmotic pump tablets contained topiramate. *PLOS ONE*; 17: e0264457.
44. Salatin S, Alami-Milani, Mitra, Cilvegar, Hamit, Fereidouni, Saber, Maghsoodi, Maryam, Monajemzadeh, Farnaz, et al. (2022). Development and Characterization of Bilayered Tablets of Diazepam for Oral Drug Delivery: Design, Optimization and In Vitro Evaluation. *Therapeutic Delivery*; 13:221–31.

Copyright: © 2025 Author. This is an open access article distributed under the Creative Commons Attribution License, which permits unrestricted use, distribution, and reproduction in any medium, provided the original work is properly cited.